Characterization of moisture in acetylated and propionylated radiata pine using low-field nuclear magnetic resonance (LFNMR) relaxometry

Beck, Greeley; Thybring, Emil Engelund; Thygesen, Lisbeth Garbrecht; Hill, Callum

Published in:
Holzforschung

DOI:
10.1515/hf-2017-0072

Publication date:
2018

Document version
Publisher's PDF, also known as Version of record

Document license:
Other

Citation for published version (APA):
Beck, G., Thybring, E. E., Thygesen, L. G., & Hill, C. (2018). Characterization of moisture in acetylated and propionylated radiata pine using low-field nuclear magnetic resonance (LFNMR) relaxometry. *Holzforschung*, *72*(3), 225-233. https://doi.org/10.1515/hf-2017-0072

Greeley Beck*, Emil Engelund Thybring, Lisbeth Garbrecht Thygesen and Callum Hill

Characterization of moisture in acetylated and propionylated radiata pine using low-field nuclear magnetic resonance (LFNMR) relaxometry

https://doi.org/10.1515/hf-2017-0072
Received May 11, 2017; accepted September 27, 2017; previously published online October 21, 2017

Abstract: Moisture in radiata pine (*Pinus radiata* D. Don) earlywood (EW), which was acetylated or propionylated to various degrees, was measured by low-field nuclear magnetic resonance (LFNMR) relaxometry. Spin-spin relaxation times (T_2) were determined for fully saturated samples at 22 and –18°C. T_2 values for EW lumen water increased with increasing acetylation weight percentage gain (WPG), perhaps caused by the less hydrophilic acetylated wood (AcW) surface. Cell wall water (W_{CW}) and the water in pits and small voids also showed increasing T_2 values as a function of WPG but with a weaker tendency. A possible explanation is the counteracting effects of decreased hydrophilicity and reduced moisture content (MC) of these water populations at higher levels of acetylation. The evaluation of propionylation on W_{CW} T_2 data was complicated by peak splitting in the relaxation spectrum. Constant T_2 values for void water populations at various WPG levels for propionylated samples indicate a modification gradient in the cell wall. Fiber saturation point (FSP) was significantly reduced by both modifications. Slightly higher FSP values for propionylated samples suggest that physical bulking is not the only factor causing moisture exclusion in AcW. But this interpretation is tentative because of the possibility of cell wall damage caused by propionylation.

Keywords: acetylation, cryo-relaxometry, fiber saturation point (FSP), low-field nuclear magnetic resonance (LFNMR), modified wood, moisture content, propionylation, spin-spin relaxation time (T_2)

***Corresponding author: Greeley Beck,** Forest and Forest Resources, Norwegian Institute of Bioeconomy Research (NIBIO), PO Box 115, NO-1431 Ås, Norway; and Department of Natural Resources Management, Norwegian University of Life Sciences, PO Box 5003, NO-1432 Ås, Norway, Tel.: +47 951 33 461, e-mail: greeley.beck@nibio.no
Emil Engelund Thybring and Lisbeth Garbrecht Thygesen: Department of Geosciences and Natural Resource Management, University of Copenhagen, Rolighedsvej 23, DK-1958 Frederiksberg C, Denmark
Callum Hill: Norwegian Institute of Bioeconomy Research (NIBIO), PO Box 115, NO-1431 Ås, Norway

Introduction

Water interactions within the wood cell wall have a substantial impact on the durability of the material, both physically and biologically. The hygroscopic wood polymers readily absorb moisture from their environment, causing undesirable dimensional changes (Glass and Zelinka 2010) and an increased risk of biological degradation (Zabel and Morrell 1992; Ibach 2005).

An effective technique for mitigating these moisture related issues is acetylation. This process chemically modifies wood in a reaction with acetic anhydride, leading to substitution of the accessible polar hydroxyl (OH) groups of wood polymers with less-polar acetyl groups. Thus, in acetylated wood (AcW) the opportunities for hydrogen bonding are reduced and physical bulking of the cell wall occurs (Rowell 2005; Hill 2007). AcW shows an increased resistance to fungal decay, and 18–20% weight percentage gain (WPG) after acetylation provides effective protection against most types of fungal decay (Goldstein et al. 1961; Peterson and Thomas 1978; Beckers et al. 1994; Mohebby 2003; Hill 2007; Rowell and Dickerson 2014). However, the exact mechanism by which acetylation imparts this protection is less well understood. Several theories have been proposed, but it seems most likely that protection results from the lower cell wall moisture content (MC) of AcW, which impedes the transport of degrading agents within the cell wall (Hill 2009; Ringman et al. 2014; Zelinka et al. 2016). Therefore, quantification and characterization of moisture within the cell wall is critical to learning more about decay resistance in AcW.

Low-field nuclear magnetic resonance (LFNMR), also known as time-domain NMR (TDNMR), is a rapid and versatile way to investigate water in the cell wall. This method assesses the relaxation time of the hydrogen nuclei in water molecules after excitation by a radio frequency pulse. The relaxation times are differentiated as T_1 (spin-lattice) and T_2 (spin-spin) relaxation. With respect to wood-water interactions, previous LFNMR research has primarily

focused on T_2 relaxation (Flibotte et al. 1990; Araujo et al. 1992; Labbé et al. 2002, 2006; Elder et al. 2006; Thygesen and Elder 2008; Thygesen et al. 2010; Telkki et al. 2013; Fredriksson and Thygesen 2017; Li et al. 2017), while a few studies have employed two-dimensional (2D) T_1T_2 LFNMR correlation spectroscopy (Cox et al. 2010; Bonnet et al. 2017), which appears to be an even more powerful method for moisture characterization.

The hydrogen nuclei of water molecules in more constricted chemical and physical environments, such as those in wood, have shorter T_2 relaxation times, and thus different water states (populations) are reflected by different T_2 values. The signal from the hydrogen nuclei in wood polymers decays very rapidly, on the order of tens of microseconds (Hsi et al. 1977; Riggin et al. 1979) and therefore can be readily distinguished from the signal of water nuclei, which relax on the order of milliseconds to seconds. The signal from the wood molecular components can be excluded by means of the Carr-Purcell-Meiboom-Gill (CPMG) pulse sequence (Carr and Purcell 1954; Meiboom and Gill 1958) and the resulting signal decay curve contains only information about the various water populations.

When the decay signal is transformed into a continuous distribution of exponentials, the water populations are visible as peaks. The peak with the fastest relaxation time has been attributed to cell wall water (W_{CW}), based on the observation that its T_2 is constant and unaffected by MC changes above the fiber saturation point (FSP) (Araujo et al. 1992). However, below FSP, both the T_2 value (Menon et al. 1987; Araujo et al. 1994; Almeida et al. 2007) and signal amplitude (Araujo et al. 1992) of this population decrease with decreasing MC. In addition to the W_{CW} peak, previous CPMG studies on softwoods identified two to three other peaks in water saturated or green samples, which represent free water in various macro-void spaces of wood (Menon et al. 1987; Flibotte et al. 1990; Araujo et al. 1992, 1994; Labbé et al. 2002, 2006; Thygesen and Elder 2008; Telkki et al. 2013; Kekkonen et al. 2014; Fredriksson and Thygesen 2017). Void size has a strong effect on T_2 relaxation, causing liquid water in smaller voids to have a shorter T_2 (Brownstein and Tarr 1979; Menon et al. 1987; Almeida et al. 2007). Therefore, the void water (W_{void}) peaks are highly variable for different wood species because they are affected by the wood cell anatomy. Two peaks were found in sapwood of Western red cedar (*Thuja plicata* Donn ex D. Don) at relaxation times of 20–100 ms and 100–300 ms (Menon et al. 1987; Flibotte et al. 1990), two to three peaks for maritime pine (*Pinus pinaster* Aiton) in the range of 10–500 ms (Labbé et al. 2002, 2006), three peaks for Scots pine (*Pinus sylvestris* L.) in the range of 10–100 ms (Kekkonen et al. 2014), and three peaks for Norway spruce (*Picea abies* (L) H. Karst) in the range of 10–1000 ms (Thygesen and Elder 2008; Fredriksson and Thygesen 2017). In studies, where three W_{void} peaks were observed, the samples were water saturated (Labbé et al. 2006; Thygesen and Elder 2008; Kekkonen et al. 2014). The peak with the longest T_2 (100–1000 ms) likely results from residual surface water (Fredriksson and Thygesen 2017). Concerning the two other W_{void} peaks, the one with the shorter T_2 has traditionally been assigned to water in latewood (LW) lumen and ray cells, and the other to earlywood (EW) lumina (Menon et al. 1987). Fredriksson and Thygesen (2017) quantified wood anatomical details and assigned LFNMR water populations of *P. abies* to EW and LW separately. The authors attributed one peak to water in EW tracheid lumina and the other to water in bordered pits, and, depending on the curve-fit approach, also to ray lumina.

The same quantitative LFNMR approach of Fredriksson and Thygesen (2017) is also suited for MC determination. When the decay signal is transformed to a continuous distribution of exponentials, the integral of a peak in the relaxation time distribution corresponds to the number of nuclei in that environment (Forshult 2004). If the total MC is determined gravimetrically, the single component MC_i is:

$$MC_i = MC\left(\frac{S_i}{S_{tot}}\right) \quad (1)$$

where S_i is the integral of the peak of moisture component i and S_{tot} is the total integral of all the peaks. Based on this approach, Telkki et al. (2013) determined the FSP of Corsican pine (*Pinus nigra* Arnold) to be 31%. This value is substantially lower than the FSP of 38.5% determined for this species by solute exclusion (Hill et al. 2005). Telkki et al. (2013) attributed the difference to the fast exchange between free water and bound water components. They also measured samples below the freezing point of water and thus obtained a signal from only the bound water population. Based on the integral of this peak, the FSP was found to be 35%, which is closer to the value determined by solute exclusion.

The role of the bulking effect of the substituents in AcW can be studied via comparison with wood modified by anhydrides with longer carbon chains, e.g. propionic anhydride (Papadopoulos and Hill 2002, 2003; Papadopoulos et al. 2010). The present work focusses on the comparison of LFNMR observations of AcW and propionylated wood (PrW) at various WPG levels. Relaxation data were collected at 22°C and –18°C for unmodified *Pinus radiata* wood (UnW) and AcW and compared to 22°C data for PrW.

Materials and methods

Materials: Eight *Pinus radiata* D. Don boards were initially cut in the transverse direction to produce 10 mm thick slices. Samples from the EW portion of the growth rings were punched out by means of a 6 mm diameter steel hole punch. These samples fit the dimensions of the NMR probe. One sample from each board was left unmodified, while six other samples were distributed among three different treatment levels (low, medium and high) for each modification, providing eight replicates (one from each board) for each treatment level.

The cylindrical samples were labeled and extracted with acetone for 6 h in a 250 ml Soxhlet apparatus equipped with single coil condenser and then dried for 18 h at 103°C and weighed. The samples were then submerged in acetic anhydride (Merck, Billerica, MA, USA, 98.5%+) or propionic anhydride (Merck, Billerica, MA, USA, 98%+) and held in the liquid under plastic netting and weights. While submerged, a 2 kPa vacuum was applied for 2 h. After vacuum release, the samples were left in the vessel for 24 h. The impregnated samples were then transferred to a reaction flask containing 500 ml of the corresponding anhydride solution, which was preheated to 110°C in an oil bath. The samples were kept in the solutions for different times to obtain a range of WPG values. Propionic anhydride modification proceeds slower and the WPG is less predictable than in case of acetylation (Hill and Jones 1996; Hill et al. 1998). Thus, more experiments were needed to obtain the whole WPG range for PrW. The reaction was quenched by pouring off the hot anhydride solution and adding 250 ml of room temperature acetone to the reaction flask. After 30 min in acetone, the samples were extracted again in the same Soxhlet apparatus with a mixture of toluene/acetone/methanol (4:1:1, v/v) for 6 h. The samples were then dried for 18 h at 103°C and weighed. The PrW samples were selected such that they had comparable WPG data to those of the AcW samples. The UnW control samples also received the same extraction procedure and were dried twice for 18 h at 103°C, but were not reacted with anhydride.

After final drying, the samples were evacuated (faucet aspirator for 1 h) and then deionized water was added under vacuum. The water contained 0.05% sodium azide to prevent any biological activity. Then, the vacuum was released and the samples were left under atmospheric pressure for 3 weeks.

NMR measurement: A Bruker mq20 minispec instrument with a 0.47 T permanent magnet (Bruker, Billerica, MA, USA) was used to perform the NMR measurements. The water saturated samples were dabbed on a wet cloth to remove any surface water without sample drying and then they were placed in pre-weighed glass NMR tubes. A Teflon rod with dimensions filling the remaining air space in the tube was then inserted to limit evaporation. This set up was then weighed before measurement. The probe region of the NMR was stabilized at 22°C (BVT 3000 nitrogen temperature control unit of Bruker, Billerica, MA, USA). The sample was allowed to equilibrate in the instrument for 2 min before measurement. The CPMG pulse sequence was used to measure the T_2 time with a pulse separation (τ) of 0.1 ms, 32 000 echoes, gain 74 dB, 16 scans and a recycle delay of 5 s. The measurements at 22°C were performed on UnW, AcW and PrW. After removal from the NMR tube, the UnW and AcW samples were wrapped in parafilm and placed in a freezer at –18°C and kept there overnight. The frozen samples were then unwrapped and placed in NMR tubes, which had been stored in the same freezer. The tube was then capped with a plastic lid and placed in the instrument, where the probe temperature was set to –18°C, and allowed to equilibrate in the instrument for 5 min before measurement. The parameters for the CPMG pulse sequence were the same as those mentioned previously. The sample mass after LFNMR measurement was determined again. The final weights were approximately 1% lower than initial weights, probably due to the loss of surface water, which remained in the NMR tube after the 22°C measurement.

Data analysis: Multi-exponential fitting is notorious for its ill-posed character and sensitivity to noise; thus, such data should be considered with caution. Although fitting more components may lead to greater accuracy, accuracy itself does not necessarily imply any physical meaning. The CPMG decay curves were analysed by (1) discrete multi-exponential fitting (Pedersen et al. 2002) performed in MATLAB (MATLAB R2015a, MathWorks, Inc., Natick, MA, USA) and (2) continuous non-negative least squares (NNLS) fitting (Lawson and Hanson 1974; Whittall et al. 1991) using PROSPA 3.2 (Magritek, Aachen, Germany). Discrete multi-exponential fitting was performed with up to five components fitted to:

$$y = C_1 e^{\frac{t}{T_{2,1}}} + \ldots + C_n e^{\frac{t}{T_{2,n}}} + C_{n+1} \quad (2)$$

Residual analysis showed that fitting five components only marginally reduced residual sum of squares, so four components were considered to be sufficient. For the frozen samples, the data were fit to only one component. The NNLS fitting in PROSPA provides a continuous distribution of T_2 values. The range for these values was set to 0.2–7000 ms and 100 data points were determined. The software also allows for selection of a smoothing parameter, which determines the magnitude of regularization for the fit. Ideally, the chosen smoothing parameter should provide a fit, which gives a mean standard deviation (SD) of residuals that matches the SD of the noise of the instrument. The noise of the measurements was determined based on the SDs of the last 100 baseline points from the CPMG decay curve, providing a value of 0.11 (a.u.). However, due to the noise statistics of the data, the mean SDs of residuals for fitting were found to plateau above this value for all analyses, ranging from 0.13 to 0.17 (a.u.). Plateau α values gave T_2 distributions with three very broad peaks, contradicting the multi-exponential discrete fitting results. Thus, a smoothing parameter of 0.1 was selected so that T_2 distributions showed four peaks for almost all spectra. The same parameter was used in all analyses because optimization based on residual statistics was not possible. For each peak, both T_2 values corresponding to maximum peak intensity and peak areas were determined.

Statistical analyses were performed using R Studio (R Studio, Inc., Boston, MA, USA). The T_2 values and MCs of each peak/component were compared among the different treatment levels by analysis of variance (ANOVA) for each fitting method separately. When significant differences ($P < 0.05$) were found, a post-hoc Tukey's honest significant difference (HSD) test was performed.

Hydroxyl group accessibility (OH_{acc}): OH_{acc} values were determined by deuterium exchange for UnW, AcW and PrW according to Beck et al. (2017). The method is based on dry mass increase after continuous exposure to deuterium oxide.

Determination of FSP: FSP values were determined from relative peak area (NNLS) of W_{CW} according to Telkki et al. (2013). For modified

samples, the FSP was determined on a dry, unreacted wood mass basis (Hill 2008). FSP values were calculated for 22°C signals by Eq. 1. At –18°C, the only signal present arises from W_{CW}, because free water will be frozen and, thus, relaxes too quickly to be detected with the CPMG measurement. Therefore, this total signal can be related to that of the 22°C measurement for FSP determination. The magnitude of NMR signal intensity is inversely proportional to temperature, and thus this temperature dependence must be accounted for (Telkki et al. 2013). Frozen signal values were therefore normalized to 22°C to calculate FSP:

$$\mathrm{FSP} = \mathrm{MC}\left(\frac{S_{\mathrm{tot},fz}\left(\frac{T_{fz}}{T_{rt}}\right)}{S_{\mathrm{tot},rt}}\right) \quad (3)$$

where MC is total moisture content obtained gravimetrically on an unreacted wood mass basis, $S_{\mathrm{tot},fz}$ is the total frozen peak area (a.u.), T_{fz} is the frozen temperature in Kelvin, T_{rt} is the room temperature (22°C) in Kelvin and $S_{\mathrm{tot},rt}$ is the total peak area measured at 22°C (a.u.).

Results and discussion

Water in cell walls

Figure 1 shows NNLS continuous T_2 distributions, where gray filled areas represent mean values with SDs and bars represent components of discrete multi-exponential fitting for UnW and AcW measured at 22 and –18°C. Tables specifying mean peak T_2 values and relative peak areas/component amplitudes are provided in the supplement. The 22°C T_2

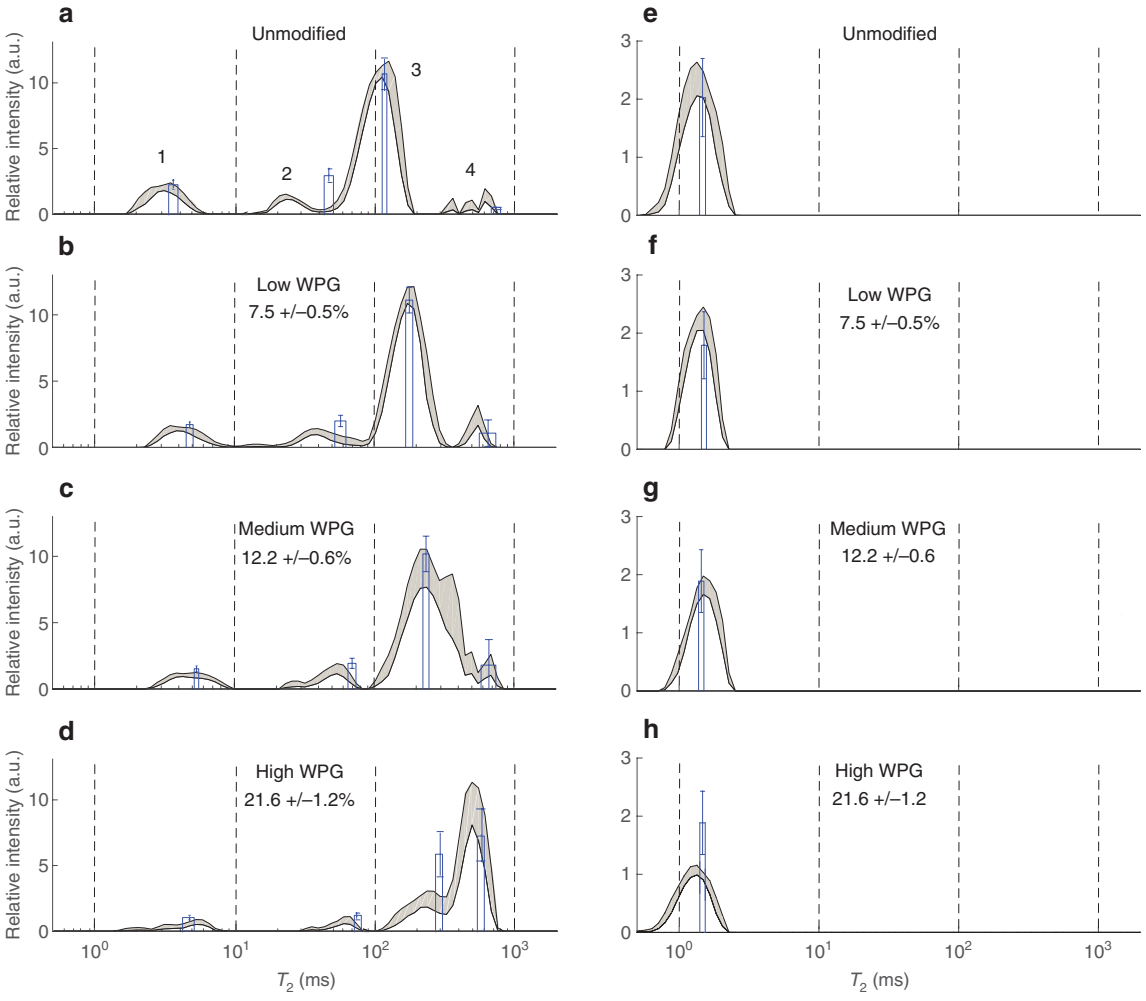

Figure 1: Continuous T_2 distributions (with peak numbers 1, 2, 3 and 4) and four component discrete fits (bars) are presented for unmodified (a, e) and acetylated (b–d, f–h) *Pinus radiata* EW measured at 22°C (a–d) and –18°C (e–h).
Gray filled areas of continuous distributions and widths of bars show mean values including SDs. Discrete component error bars show the standard deviation of the component amplitude and are placed at the mean component T_2 value. Please note the different scales on the ordinate axes in (a–d) and (e–f).

values determined from continuous fitting are more variable than those of discrete fitting, but both show similar trends. Peak 1 T_2 values have been assigned to cell wall water (W_{CW}) (Menon et al. 1987; Araujo et al. 1992, 1994; Labbé et al. 2002; Thygesen and Elder 2008; Kekkonen et al. 2014; Telkki et al. 2013; Fredriksson and Thygesen 2017). AcW shows significantly longer T_2 values for this peak compared to UnW, but increasing levels of acetylation did not significantly increase T_2 (Figure 2a). Removal of hemicelluloses leads to longer T_2 values for W_{CW} (Elder and Houtman 2013). It is possible that the degree of hemicellulose acetylation at low and high WPG is similar as hemicelluloses are rapidly acetylated (Rowell et al. 1994). If interaction with hemicelluloses is the determining factor for W_{CW} T_2 relaxation, this may explain similar values between low and high WPGs.

Alternatively, the amount of W_{CW} may also play a role in decreasing T_2 values of peak 1. Below FSP, W_{CW} T_2 relaxation decreases with decreasing MC (Menon et al. 1987; Araujo et al. 1994; Almeida et al. 2007). The MC associated with the W_{CW} peak is also significantly reduced at higher WPGs (Figure 1). However, at higher levels of acetylation, more OH groups are substituted and the wood becomes less hydrophilic, as illustrated by the reduced OH_{acc} determined with deuterium exchange (Figure 2). Lower hydrophilicity means less affinity of water for the wood surface and thus longer T_2 relaxation time (Mitchell et al. 2005). This effect may compensate for T_2 reduction resulting from decreased MC. Thus, AcW with high WPG could have similar T_2 values for W_{CW} compared with AcW with low WPG.

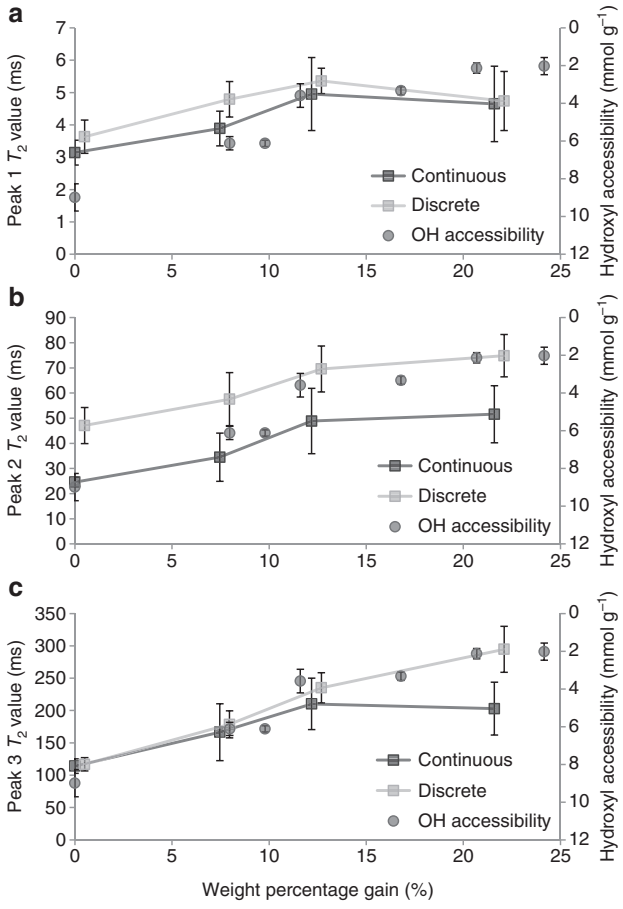

Figure 2: Mean T_2 values (from continuous T_2 distributions and discrete fits) as a function of WPG of AcW (*Pinus radiata* EW). WPG values for discrete fitting are shifted by 0.25% to prevent data points from overlapping. Hydroxyl accessibility values determined from deuterium exchange are also presented for UnW and AcW (Beck et al. 2017).

Water in voids

Water populations in the wood void structure (W_{void}) are represented by peaks 2 and 3 (Figure 1). Peak 4 is due to residual surface water left on the sample after wet cloth dabbing (Fredriksson and Thygesen 2017). Peak 4 T_2 values are therefore independent of the acetylation degree (ANOVA, $P > 0.05$). The other two W_{void} peaks are also similar to results from Fredriksson and Thygesen (2017) because that study measured EW separated from LW as was done here. Peak 3 T_2 values in UnW correspond well with data in the aforementioned study assigned to W_{void} in EW tracheid lumena (94 ± 10 ms obtained by continuous fitting). The slightly longer UnW T_2 of *P. radiata* observed here is probably due to the slightly larger EW tracheid diameter in *P. radiata* (45 µm, Bamber and Burley 1983) vs. *P. abies* (30–38 µm, Fredriksson and Thygesen 2017). Peak 2 T_2 values in UnW are more than double than those found by Fredriksson and Thygesen (2017), which were assigned to water in pits (10 ± 2 ms, continuous fitting). A thicker cell wall and thus greater pit depth for *P. radiata* compared *P. abies* may account for this discrepancy (Bamber and Burley 1983; Cato et al. 2006).

The W_{void} T_2 values of peaks 2 and 3 tend to increase at higher WPG levels (Figure 2b,c). Thygesen and Elder (2008) also reported increased T_2 values for lumen water for AcW. Reduced hydrophilicity increases lumen water T_2 values as seen for charring (Elder et al. 2006), furfurylation (Thygesen and Elder 2008), and thermal modification (Kekkonen et al. 2014; Javed et al. 2015). The reduction of OH_{acc} with increasing WPG seems to correlate better with peak 3 T_2 values than peak 2 T_2 values (Figure 2). However, at the high WPG levels, peak 3 T_2 values are misleading because this peak is merged with the surface water peak (Figure 1d). Peak 4 increase at high WPG is probably due to inclusion of EW lumen water in this peak. Therefore, it is likely that the peak 3 T_2 data in Figure 2c underestimate

EW lumen water T_2 relaxation at the higher WPG level. Peak 2 T_2 values tend to increase with increasing WPG up to 12% but then the data level off and remain constant up to 21% WPG. This could be due to decreased MC at high WPG levels, as was observed for the W_{CW} peak. Peak 2 MC at the high WPG level is also significantly reduced.

Fiber saturation

$FSP_{22°C}$ and $FSP_{-18°C}$ data (Eqs. 1 and 3) are illustrated in Figure 3 (continuous fitting). ANOVA and post-hoc Tukey's HSD analysis revealed that FSP values for all treatment levels are significantly different from one another for both methods of FSP determination ($P < 0.05$). Comparison of linear regression models of FSP vs. WPG for the two methods reveal that the slopes of the two models are not significantly different ($P = 0.68$), but intercepts are different ($P = 0.003$). The effect of acetylation WPG on FSP is therefore independent of the method of FSP determination, but the $FSP_{-18°C}$ data are significantly higher than the $FSP_{22°C}$ data. These differences are probably due to fast exchange between W_{CW} and W_{void} in case of 22°C measurement. Cox et al. (2010) observed such an exchange with 2D-T_2T_2 LFNMR experiments. Telkki et al. (2013) argued that water involved in W_{CW}/W_{void} exchange is included in the W_{void} populations. Thus, the 22°C W_{CW} peak and FSP values based on this signal will underrepresent W_{CW}.

The residual unfrozen water present in $FSP_{-18°C}$ measurements is unable to freeze because it is either bound to wood polymers or it is confined in cell wall nanopores. W_{void} populations are frozen at –18°C and therefore W_{CW}/W_{void} exchange does not occur. The average $FSP_{-18°C}$ of UnW is 28.9% (Eq. 3). However, this method may underestimate FSP as other studies reported 10–20% reduction in W_{CW} signal intensity for –20°C measurements compared to –3°C, possibly caused by differences in melting point depression of water confined in nanopores (Telkki et al. 2013; Gao et al. 2015). Accounting for this reduction, the average $FSP_{-18°C}$ of UnW is between 32% and 35%, which is similar to the value (35%) of Telkki et al. (2013) obtained for Scots pine sapwood.

Compared to the $FSP_{-18°C}$ of UnW, the $FSP_{-18°C}$ of AcW (21.6% WPG) was reduced by 52%. Thybring (2013) calculated this moisture exclusion efficiency (MEE) from a range of literature sources and methods and reported an average MEE value of 42% for AcW at 20% WPG. The values of the present study are slightly higher, probably due to the different wood species and the selective observations on EW. At the high WPG level, the average fully saturated cell wall MC is 14%. The threshold MC for fungal degradation is 20% (Eaton and Hale 1993), while 18–20% threshold acetylation WPG is needed for effective protection. If the $FSP_{-18°C}$ vs. WPG linear regression model is scaled to higher values by 15% to compensate for frozen cell wall water at –18°C due to melting point depression differences as previously described, the predicted FSP value at 18% WPG level (WPG protection threshold) is 21% MC. Accordingly, acetylation provides decay protection by reducing cell wall MC below the decay threshold MC at the protection threshold WPG.

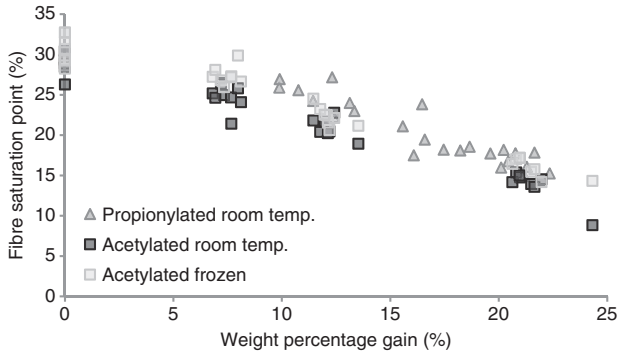

Figure 3: FSP data of UnW, AcW and PrW calculated from continuous T_2 distribution peak areas.
PrW data were obtained at 22°C, while those of AcW both at 22°C and –18°C.

Comparison of modifications

FSP data of PrW and AcW are presented in Figure 3. Comparison of linear regression models for $FSP_{22°C}$ vs. WPG show significantly different slopes for PrW and AcW ($P = 0.016$), while intercepts were not significantly different ($P = 0.64$). The significantly larger FSP reduction in AcW implies that physical cell wall bulking is not solely responsible for reduced cell wall MC in AcW. Papadopoulos and Hill (2003) compared vapor sorption isotherms of AcW to wood samples reacted with a range of larger carboxylic acid anhydrides and found only insignificant differences between modifications. The comparability, however, is complicated by the fact that the authors used pyridine as a swelling agent during wood modifications as pyridine is a strong swelling solvent, which may lead to a similar degree of cell wall damage for AcW and the long chain substituents. In the present study, without a swelling agent, cell wall damage in the PrW samples can be assumed, which leads to more water inclusion and thus higher FSP data. Beck et al. (2017) also found increased OH_{acc} in PrW modified without a swelling agent and attributed this to damage. As the extent of cell wall damage in PrW samples unknown, the PrW FSP results should be interpreted with

caution. Relaxation spectra and further discussion of T_2 values for PrW samples are provided in the supplement.

Conclusions

Cell wall water (W_{CW}) T_2 values in AcW at 22°C are significantly higher than those of unmodified wood (UnW), and higher levels of acetylation do not further increase T_2. The combined effect of lower hydrophilicity and cell wall MC may explain the results. FSP was determined based on W_{CW} relative peak areas measured at 22°C and –18°C. The slightly lower values of the former were interpreted as a result of exchange between W_{CW} and void volume water (W_{void}). In both cases, a linear decrease in FSP was seen with increasing acetylation degree as measured by WPG. The linear regression model of FSP vs. WPG based on –18°C measurements for AcW was interpreted such that cell wall MC is reduced below the decay threshold MC at WPG values thought to provide effective protection against most types of fungal decay. PrW shows constant T_2 values for increasing levels of WPG either due to a modification gradient within the cell wall or cell wall damages. Like acetylation, propionylation also linearly reduced FSP but with a lower slope. A possible interpretation is that physical bulking is not the only mechanism by which acetylation excludes moisture in wood. However, the propionylation reaction may have damaged the cell wall more than acetylation so this conclusion is uncertain. The complications of cell wall damage and modification gradients could be avoided by the application of swelling agents, e.g. pyridine, during the modification reactions, but such agents are not used in industrial acetylation procedures.

Acknowledgments: The authors gratefully acknowledge Gry Alfredsen for helpful discussions during planning and execution of experiments. G. Beck also thanks the Norwegian Institute for Bioeconomy Research for internal PhD funding, grant numbers 395602 and 335200-3. E.E. Thybring gratefully acknowledges funding from the VILLUM FONDEN postdoc programme.

Author contributions: All the authors have accepted responsibility for the entire content of this submitted manuscript and approved submission.
Research funding: Norwegian Institute for Bioeconomy Research for internal PhD funding, grant numbers 395602 and 335200-3; VILLUM FONDEN postdoc programme.
Employment or leadership: None declared.
Honorarium: None declared.

References

Almeida, G., Gagné, S., Hernández, R.E. (2007) A NMR study of water distribution in hardwoods at several equilibrium moisture contents. Wood Sci. Technol. 41:293.

Araujo, C.D., MacKay, A.L., Hailey, J.R.T., Whittall, K.P., Le, H. (1992) Proton magnetic resonance techniques for characterization of water in wood: application to white spruce. Wood Sci. Technol. 26:101–113.

Araujo, C.D., Avramidis, S., MacKay, A.L. (1994) Behaviour of solid wood and bound water as a function of moisture content. A Proton Magnetic Resonance Study. Holzforschung 48:69–74.

Bamber, R., Burley, J. The Wood Properties of Radiata Pine. Farnham Royal, London, 1983.

Beck, G., Strohbusch, S., Erik Larnøy, E., Militz, H., Hill, C. (2017) Accessibility of hydroxyl groups in anhydride modified wood as measured by deuterium exchange and saponification. Holzforschung 72:17–23.

Beckers, E.P.J., Militz, H., Stevens, M. Resistance of Acetylated Wood to Basidiomycetes, Soft Rot and Blue Stain. The International Research Group on Wood Protection, Stockholm. IRG/WP 94-40021, 1994.

Bonnet, M., Courtier-Murias, D., Faure, P., Rodts, S., Care, S. (2017) NMR determination of sorption isotherms in earlywood and latewood of Douglas fir. Identification of bound water components related to their local environment. Holzforschung 71:481–490.

Brownstein, K.R., Tarr, C.E. (1979) Importance of classical diffusion in NMR studies of water in biological cells. Phys. Rev. A. 19:2446–2453.

Carr, H.Y., Purcell, E.M. (1954) Effects of diffusion on free precession in nuclear magnetic resonance experiments. Phys. Rev. 94:630–638.

Cato, S., McMillan, L., Donaldson, L., Richardson, T., Echt, C., Gardner, R. (2006) Wood formation from the base to the crown in Pinus radiata: gradients of tracheid wall thickness, wood density, radial growth rate and gene expression. Plant Mol. Biol. 60:565–581.

Cox, J., McDonald, P.J., Gardiner, B.A. (2010) A study of water exchange in wood by means of 2D NMR relaxation correlation and exchange. Holzforschung 64:259–266.

Eaton, R.A., Hale, M.D.C. Wood: Decay, Pests and Protection. Chapman and Hall, London, 1993.

Elder, T., Houtman, C. (2012) Time-domain NMR study of the drying of hemicellulose extracted aspen (*Populus tremuloides* Michx.). Holzforschung 67:405–411.

Elder, T., Labbé, N., Harper, D., Rials, T. (2006) Time domain-nuclear magnetic resonance study of chars from southern hardwoods. Biomass Bioenerg. 30:855–862.

Flibotte, S., Menon, R.S., MacKay, A.L., Hailey, J.R.T. (1990) Proton magnetic resonance of Western red cedar. Wood Fiber Sci. 22:362–376.

Forshult, S.E. Quantitative analysis with pulsed NMR and the CONTIN computer program. Karlstad University Studies, Karlstad, Sweden 2004.

Fredriksson, M., Thygesen, L.G. (2017) The states of water in Norway spruce (Picea abies (L.) Karst.) studied by low-field nuclear magnetic resonance (LFNMR) relaxometry: assignment of free-water populations based on quantitative wood anatomy. Holzforschung 71:77–90.

Gao, X., Zhuang, S., Jin, J., Cao, P. (2015) Bound water content and pore size distribution in swollen cell walls determined by NMR technology. BioResources 10:8208–8224.

Glass, S.V., Zelinka, S.L. (2010) Moisture relations and physical properties of wood. In: Wood Handbook, Wood as an Engineering Material. General Technical Report FPL-GTR-190. U.S. Department of Agriculture, Forest Service, Forest Products Laboratory, Madison, WI.

Goldstein, I.S., Jeroski, E.B., Lund, A.E., Nielson, J.F., Weaver, J.W. (1961) Acetylation of wood in lumber thickness. Forest Prod. J. 11:363–370.

Hill, C.A.S. Wood Modification: Chemical, Thermal and Other Processes. John Wiley & Sons, West Sussex, England, 2007.

Hill, C.A.S. (2008) The reduction in the fibre saturation point of wood due to chemical modification using anhydride reagents: a reappraisal. Holzforschung 62:423–428.

Hill, C.A.S. (2009) Why does acetylation protect wood from microbiological attack? Wood Mater. Sci. Eng. 4:37–45.

Hill, C.A.S., Jones, D. (1996) A chemical kinetics study of the propionic anhydride modification of corsican pine. (1): Determination of activation energies. J. Wood Chem. Technol. 16:235–247.

Hill, C.A.S., Jones, D., Strickland, G., Cetin, N.S. (1998) Kinetic and mechanistic aspects of the acetylation of wood with acetic anhydride. Holzforschung 52:623–629.

Hill, C.A.S., Forster, S.C., Farahani, M.R.M., Hale, M.D.C., Ormondroyd, G.A., Williams, G.R. (2005) An investigation of cell wall micropore blocking as a possible mechanism for the decay resistance of anhydride modified wood. Int. Biodeter. Biodegr. 55:69–76.

Hsi, E., Hossfeld, R., Bryant, R.G. (1977) Nuclear magnetic resonance relaxation study of water absorbed on milled northern white-cedar. J. Colloid. Interf. Sci. 62:389–395.

Ibach, R.E. 2005. Biological properties of wood. In: Handbook of Wood Chemistry and Wood Composites. Ed. Rowell, R.M. CRC Press, Boca Raton, USA, pp. 99–120.

Javed, M.A., Kekkonen, P.M., Ahola, S., Telkki, V.-V. (2015) Magnetic resonance imaging study of water absorption in thermally modified pine wood. Holzforschung 69:899–907.

Kekkonen, P.M., Ylisassi, A., Telkki, V.-V. (2014) Absorption of water in thermally modified pine wood as studied by nuclear magnetic resonance. J. Phys. Chem. C. 118:2146–2153.

Labbé, N., De Jéso, B., Lartigue, J-C., Daudé, G., Pétraud, M., Ratier, M. (2002) Moisture content and extractive materials in maritime pine wood by low field 1H NMR. Holzforschung 56:25–31.

Labbé, N., De Jéso, B., Lartigue, J-C., Daudé, G., Pétraud, M., Ratier, M. (2006) Time-domain 1H NMR characterization of the liquid phase in greenwood. Holzforschung 60:265–270.

Lawson, C.L., Hanson, R.J. Linear Least Squares with Linear Inequality Constraints. Solving Least Squares Problems. Prentice-Hall, Englewood Cliffs, USA, 1974.

Li, X., Gao, Y., Zhang, M., Wang, X., Wei, X. (2017) Water migration in poplar wood during microwave drying studied by time domain nuclear magnetic resonance (TD-NMR). Holzforschung 71:881–887.

Meiboom, S., Gill, D. (1958) Modified spin-echo method for measuring nuclear relaxation times. Rev. Sci. Instrum. 29:688–691.

Menon, R.S., MaCkay, A.L., Hailey, J.R.T., Bloom, M., Burgess, A.E., Swanson, J.S. (1987) An NMR determination of the physiological water distribution in wood during drying. J. Appl. Polym. Sci. 33:1141–1155.

Mitchell, J., Stark, S.C., Strange, J.H. (2005) Probing surface interactions by combining NMR cryoporometry and NMR relaxometry. J. Phys. D Appl. Phys. 38:1950.

Mohebby, B. Biological attack of acetylated wood. PhD thesis. Institute of Wood Biology and Wood Technology, Georg-August-Universität Göttingen, Göttingen, Germany 2003.

Papadopoulos, A.N., Hill, C.A.S. (2002) The biological effectiveness of wood modified with linear chain carboxylic acid anhydrides against *Coniophora puteana*. Holz Roh Werkst. 60:329–332.

Papadopoulos, A.N., Hill, C.A.S. (2003) The sorption of water vapour by anhydride modified softwood. Wood Sci. Technol. 37:221–231.

Papadopoulos, A.N., Militz, H., Pfeffer, A. (2010) The biological behaviours of pine wood modified with linear chain carboxylic acid anhydrides against soft rot fungi. Int. Biodeter. Biodegr. 64:409–412.

Pedersen, H.T., Bro, R., Engelsen, S.B. (2002) Towards rapid and unique curve resolution of low field NMR relaxation data: trilinear SLICING versus two-dimensional curve fitting. J. Magn. Reson. 157:141–155.

Peterson, M.D., Thomas, R.J. (1978) Protection of wood from decay fungi by acetylation – an ultrastructural and chemical study. Wood Fiber Sci. 10:149–163.

Riggin, M.T., Sharp, A.R., Kaiser, R., Schneider, M.H. (1979) Transverse NMR relaxation of water in wood. J. Appl. Polym. Sci. 23:3147–3154.

Ringman, R., Pilgård, A., Brischke, C., Richter, K. (2014) Mode of action of brown rot decay resistance in modified wood: a review. Holzforschung 68:239–246.

Rowell, R.M. Handbook of Wood Chemistry and Wood Composites. CRC Press, Boca Raton, USA, 2005.

Rowell, R., Dickerson, J. (2014) Acetylation of wood. In: Deterioration and Protection of Sustainable Biomaterials. Eds. Schultz, T., Goodell, B., Nicholas, D. ACS Symposium Series 1158. American Chemical Society, pp. 301–327.

Rowell, R.M., Simonson, R., Hess, S., Plackett, D.V., Cronshaw, D., Dunningham, E. (1994) Acetyl distribution in acetylated whole wood and reactivity of isolated wood cell-wall components to acetic anhydride. Wood Fiber Sci. 26:11–18.

Telkki, V.-V., Yliniemi, M., Jokisaari, J. (2013) Moisture in softwoods: fiber saturation point, hydroxyl site content, and the amount of micropores as determined from NMR relaxation time distributions. Holzforschung 67:291–300.

Thybring, E.E. (2013) The decay resistance of modified wood influenced by moisture exclusion and swelling reduction. Int. Biodeter. Biodegr. 82:87–95.

Thygesen, L., Elder, T. (2008) Moisture in untreated, acetylated, and furfurylated Norway spruce studied during drying using time domain NMR. Wood Fiber Sci. 40:309–320.

Thygesen, L.G., Engelund, E.T., Hoffmeyer, P. (2010) Water sorption in wood and modified wood at high values of relative humidity.

Part I: results for untreated, acetylated, and furfurylated Norway spruce. Holzforschung 64:315–323.
Whittall, K.P., Bronskill, M.J., Henkelman, R.M. (1991) Investigation of analysis techniques for complicated NMR relaxation data. J. Magn. Reson. 95:221–234.
Zabel, R.A., Morrell, J.J. Wood Microbiology: Decay and its Prevention. Academic Press, San Diego, USA, 1992.
Zelinka, S.L., Ringman, R., Pilgård, A., Thybring, E.E., Jakes, J.E., Richter, K. (2016) The role of chemical transport in the brown-rot decay resistance of modified wood. Int. Wood Prod. J. 7:66–70.

Supplemental Material: The online version of this article offers supplementary material (https://doi.org/10.1515/hf-2017-0072).